Agricultural Water Management 323 (2026) 110092

Contents lists available at ScienceDirect

Agricultural Water Management

journal homepage: www.elsevier.com/locate/agwat

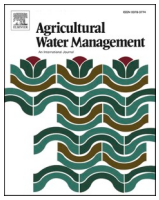

Assessing the performance of multi-timescale drought indices for monitoring agricultural drought impacts on wheat yield

Mahsa Bozorgi [a,b,*], Jordi Cristóbal [b], Jaume Casadesús [a]

[a] Efficient Use of Water in Agriculture Program, Institute of AgriFood, Research and Technology (IRTA), Fruitcentre, Parc Agrobiotech, Lleida 25003, Spain
[b] Department of Geography, Universitat Autònoma de Barcelona, Campus de Bellaterra, Edifici B, Carrer de la Fortuna, s/n, 08193 Bellaterra, Spain

ARTICLE INFO

Handling Editor: Enrique Fernández

Keywords:
Crop water stress
Remote sensing
Evapotranspiration
Precipitation

ABSTRACT

Crop yields are increasingly threatened by intensifying droughts in southern Europe, yet the long-term, spatially explicit quantification of yield response to agricultural drought remains limited. Remote sensing can address this gap by providing continuous spatiotemporal estimates of crop water stress. This study quantified the response of wheat yield to agricultural drought from 2003 to 2021 across four autonomous communities in Spain—La Rioja, Castilla y León, Castilla-La Mancha, and Andalucía—using three drought indicators, including a meteorological drought index, the Standardized Precipitation-Evapotranspiration Index (SPEI), and two remote sensing-based indices, the Standardized Precipitation-Actual Evapotranspiration Index (SPET) and the Standardized Evapotranspiration Deficit Index (SEDI), derived from a physical model that estimates actual crop evapotranspiration ($ET_{c\ act}$). Drought indices were aggregated at timescales from 1 to 12 months to identify the accumulation of timescales most relevant to wheat yield variability in each region. Results indicated that correlations varied spatially, with the strongest wheat yield–drought correlation in La Rioja ($r = 0.79$ for SPEI, 0.62 for SPET, and 0.81 for SEDI) and the weakest in Andalucía ($r \approx 0.33$–0.35). Mediterranean regions (Andalucía and Castilla-La Mancha) showed the strongest correlation at short timescales (1–3 month) during late spring, while temperate continental regions (Castilla y León and La Rioja) responded to longer timescales (3–6 month) in early summer. Among indices, SEDI exhibited the strongest and most consistent correlation with wheat yield variability. These results highlight the value of integrating remotely sensed $ET_{c\ act}$ with ERA5 reanalysis for region-specific drought monitoring, offering significant potential for advancing operational agricultural water management strategies under increasing drought frequency and climate change.

1. Introduction

Agricultural drought poses a significant threat to crop productivity and, ultimately, global food security, intensified by climate-driven water scarcity and the escalating demands of a growing global population (Leng and Hall, 2019; Marengo et al., 2017; Visser et al., 2024; Wang and Ren, 2025; Wen et al., 2025). Over the past five decades, drought-related yield reductions have contributed to global cereal production losses ranging from 4 % to 13 % (Lobell and Di Tommaso, 2025). Economically, agricultural gross domestic product (GDP) losses due to natural disasters are estimated at 3–7.5 % annually, with drought emerging as a leading driver and projected to account for nearly 35 % of total agricultural losses by 2035 (OECD, 2025). These trends underscore the critical need to understand drought impacts on agricultural productivity for adopting agricultural water management strategies as an effective way for drought mitigation impacts (García-León et al., 2019; Mahadevan et al., 2024; Wilhite and Svoboda, 2000) as well as improving crop yield prediction frameworks (Anderson et al., 2016; Jurečka et al., 2021).

This vulnerability is particularly pronounced in strategically important crops such as wheat, the most extensively cultivated and increasingly demanded cereal globally (Curtis, 2019). However, rising temperatures and increasing frequency of drought events threaten wheat productivity (Asseng et al., 2015). This challenge is particularly significant in Spain, where wheat is predominantly grown under rainfed systems and recurrent droughts associated with the Mediterranean climate pose a major risk to yield stability (Ribeiro et al., 2019; Vicente-Serrano et al., 2013, 2012; Wu et al., 2014). The magnitude of

* Corresponding author at: Efficient Use of Water in Agriculture Program, Institute of AgriFood, Research and Technology (IRTA), Fruitcentre, Parc Agrobiotech, Lleida 25003, Spain.
E-mail addresses: mahsa.bozorgi@irta.cat (M. Bozorgi), jordi.cristobal@uab.cat (J. Cristóbal), jaume.casadesus@irta.cat (J. Casadesús).

https://doi.org/10.1016/j.agwat.2025.110092
Received 1 July 2025; Received in revised form 12 December 2025; Accepted 15 December 2025
0378-3774/© 2025 The Authors. Published by Elsevier B.V. This is an open access article under the CC BY license (http://creativecommons.org/licenses/by/4.0/).

this problem becomes evident when considering that nearly 30 % of Spain's population already experiences permanent water stress, while up to 70 % is affected by seasonal water stress (European Environmental Agency (EEA) (EEA), 2024), increasingly constraining the expansion of irrigated agriculture. This context underscores the urgent need to improve our understanding of drought impacts on rainfed crop productivity, which is essential for national water and food security (Qiu et al., 2023; Rockström et al., 2010; Zampieri et al., 2017).

Understanding the dynamic of agricultural drought is fundamental to addressing these challenges. Agricultural drought occurs when meteorological drought—characterized by prolonged reduced precipitation combined with elevated atmospheric evaporative demand—propagates into root-zone moisture deficits, constraining plant water uptake, growth, and productivity (Wilhite, 2005). In water-limited regions such as Spain, where agriculture is predominantly rainfed, precipitation variability plays a critical role in crop productivity (Peña-Gallardo et al., 2019). Recent studies report a long-term decline in total rainfall across Spain, accompanied by more frequent and intense extreme precipitation events (Jiménez-Donaire et al., 2020). These shifts in precipitation patterns are especially concerning rainfed agriculture, which relies directly on rainfall (Rockström et al., 2010). Consequently, intra-annual and interannual precipitation variability are intensifying crop water stress and amplifying yield instability in Spain's rainfed agricultural systems.

Thus, to monitor and assess agricultural drought, numerous indices have been developed with different conceptual foundations (Heim, 2002; Wilhite et al., 2014). These indicators are mainly based on meteorological variables (Palmer, 1965; Vicente-Serrano et al., 2010, 2011; McKee et al., 1993; Stagge et al., 2014), hydrological components (Anderson et al., 2011; Karl, 1986; Nalbantis and Tsakiris, 2009; Shukla and Wood, 2008; Wu et al., 2021), and vegetation characteristics (Alatorre et al., 2015; Brown et al., 2008; Xu et al., 2024; Z. Xu et al., 2024). However, traditional meteorological indices present significant limitations in fully capturing crop water stress. The Palmer Drought Severity Index (PDSI), based on precipitation and temperature, is constrained by its fixed temporal resolution (Guttman, 1998; Palmer, 1965), while the Standardized Precipitation Index (SPI) addresses timescale limitations but relies solely on precipitation data (McKee et al., 1993). Since drought encompasses both reduced precipitation and increased temperature, which drives rising atmospheric evaporative demand (Beguería et al., 2014; Stagge et al., 2017), precipitation alone may be insufficient to capture crop water stress.

In order to address these limitations, the Standardized Precipitation-Evapotranspiration Index (SPEI), developed by (Vicente-Serrano et al., 2010), constitutes a multi-temporal index based on the climatic water balance between precipitation and potential evapotranspiration (ET), offering insights into both short- and long-term drought conditions (Vicente-Serrano et al., 2012, 2013; Vicente-Serrano and Beguería, 2016). Initially, potential ET was estimated using the Thornthwaite method, which relies on temperature and daylight hours. However, Beguería et al. (2014) demonstrated that using reference ET (ET_o) based on the Penman-Monteith method provided a more physically robust alternative, albeit requiring more meteorological inputs. Some studies have further proposed using actual crop evapotranspiration ($ET_{c\ act}$) instead of ET_o, arguing that the surface water balance (precipitation minus $ET_{c\ act}$) better reflects crop water availability (Richard G. Allen et al., 1998; Peng et al., 2024; Perez et al., 2024). Accordingly, (Beguería et al., 2014) suggested that replacing precipitation with $ET_{c\ act}$ (ET_o minus $ET_{c\ act}$) may enhance the accuracy of drought assessments as it better represents crop water deficits. Nevertheless, the extent to which ET-based drought indices can explain crop yield-drought variability requires further evaluation.

While $ET_{c\ act}$ represents crop water loss under actual conditions by integrating both biophysical and climatic variables, its spatial estimation presents methodological challenges. Ground-based methods such as lysimeters and eddy covariance towers provide only point-scale estimates that fail to capture the spatial heterogeneity of agricultural areas (Sun et al., 2025), limiting their utility for regional drought assessment and yield analysis. Remote sensing overcomes these limitations by offering spatially continuous, long-term observations of land surface temperature and biophysical variables, thus providing robust drought monitoring across diverse spatial and temporal scales and enhancing the accuracy of crop water stress assessments (Hu et al., 2020; Schwartz et al., 2022; West et al., 2019). Leveraging satellite-derived $ET_{c\ act}$ data thus offers a practical approach for assessing drought impacts across Spain with diverse agricultural landscapes and climatic zones.

Previous studies in Spain have explored the relationship between drought indices and vegetation variability, providing valuable insights while also revealing methodological gaps. Vicente-Serrano et al. (2006) reported that the SPI at 3–4-month timescales was most strongly correlated with NDVI and cereal yield in northeastern Spain. Peña-Gallardo et al. (2019) demonstrated that drought indices computed at multi-timescales better explained yield variability than single-timescale indicators, while García-León et al., (2019) found that satellite-derived indices outperformed meteorological indices in explaining spatial yield variability. Possega et al. (2023) similarly demonstrated that agricultural drought indices, which account for soil water balance, better captured vegetation responses than meteorological indicators. Benito-Verdugo et al. (2023) also emphasized the role of root-zone soil moisture in explaining cereal yield variability in the center of Spain (Castilla y León and Castilla–La Mancha). Khlif et al. (2023) assessed the performance of remote sensing-based drought indices in relation to rainfed cereal crops in northeastern Spain, finding that the Evapotranspiration Anomaly Index, derived from ET_o, showed the strongest correlation with wheat yield, reaching a correlation coefficient of 0.75 in July. More recently, Bellvert et al. (2025) investigated drought impacts on agricultural productivity in northeastern Spain using a remote sensing-based $ET_{c\ act}$ model, demonstrating its effectiveness in capturing spatial and temporal variations in crop yield.

Although previous studies have advanced our understanding of drought dynamics, a notable gap remains in systematically evaluating the long-term performance of both meteorological and remote sensing-based drought indices across multiple timescales against farm-level yield data in Spain. To address this gap, this study aims to calculate three drought indices, the Standardized Precipitation Evapotranspiration Index (SPEI), the Standardized Precipitation-Actual Evapotranspiration Index (SPET) and the Standardized Evapotranspiration Deficit Index (SEDI), through ET_o estimates from meteorological data (ERA5) as well as $ET_{c\ act}$ estimates from a remote sensing modelling framework and to assess them using field reports of rainfed wheat yield from 2003 to 2021 across four major wheat-producing autonomous communities in Spain, with the objective of identifying the most suitable drought index and the accumulation timescales to enhance agricultural drought monitoring and inform regional agricultural water management strategies.

Thus, to improve drought impact assessment and support more resilient agricultural water management and yield forecasting, the main study objectives are to (1) determine which drought index best explains yield response to drought and (2) identify the accumulation timescales that most effectively capture yield variability in each region.

2. Materials and methods

2.1. Wheat yield data

The ESYRCE dataset (*Encuesta sobre Superficies y Rendimientos de Cultivos* – ESYRCE - https://www.mapa.gob.es/es/estadistica/temas/estadisticas-agrarias/agricultura/esyrce/) was used to extract the winter rainfed wheat yield (including common and durum wheat). This survey has recorded crop production at the farm level since 1990.

The ESYRCE survey employs a conglomerate stratified sampling

approach, utilizing the Universal Transverse Mercator (UTM10) coordinate system to construct 10 km × 10 km grid blocks, covering the entire Spain. Each of these blocks is divided into 100 cells of 1 km × 1 km. Squared segments of 500 m to 700 m in each cell are the basic units to survey crop yields every year from May to August. In this dataset, wheat data for 2001 and 2002 were missing. Hence, to align with the ET_o estimated from meteorological data (ERA5) and $ET_{c\ act}$ dataset calculated using remote sensing and meteorological data (Aqua MODIS images and ERA5 meteorological data, see Bozorgi et al., 2024), this study covered the period from 2003 to 2021.

Wheat is one of the most widespread crops in Spain, intensively located at the central plateaus (García-León et al., 2019; Martínez-Moreno et al., 2023). Accordingly, four Spanish autonomous communities were selected for this study (Fig. 1): La Rioja, Castilla y León, Castilla-La Mancha, and Andalucía where wheat represents one of the most significant crops (Martínez-Moreno et al., 2023). In the study area, winter wheat sowing and harvesting periods vary across cultivars and regions, typically spanning from late November for sowing to July for harvesting.

2.2. Actual crop evapotranspiration ($ET_{c\ act}$)

Monthly $ET_{c\ act}$ was derived by integrating daily estimates from the Two-Source Energy Balance (TSEB) model, implemented at 1 km spatial resolution using MODIS Aqua observations combined with ERA5 meteorological data. The TSEB framework partitions the surface energy balance into soil and canopy components, estimating latent heat flux (LE) as the residual of available energy—net radiation (Rn) minus soil heat flux (G)—and sensible heat flux (H). This approach leverages remotely sensed land surface temperature, which integrates the thermal contributions of vegetation and soil and is therefore well-suited for mixed agricultural landscapes. Vegetation indices were incorporated to retrieve key biophysical variables, while land cover products were used to specify vegetation properties and surface characteristics required by the model. Further methodological details are provided in (Bozorgi et al., 2024) and in the supplementary materials.

2.3. Reference evapotranspiration (ET_o)

Daily ET_o was computed using the FAO-56 Penman–Monteith equation (Allen et al., 1998), driven by ERA5 meteorological data (incoming shortwave radiation, air temperature, actual water vapor pressure, atmospheric pressure and wind speed) at 0.25° spatial resolution. The FAO-56 formulation was applied with aerodynamic and surface resistances outlined in the FAO-56 guidelines. The methodology is detailed in (Bozorgi et al., 2024). Daily ET_o estimates were subsequently aggregated to obtain monthly ET_o values.

2.4. Precipitation

Daily precipitation data were obtained from the Spanish State Meteorological Agency (AEMET), which operates over 2000 stations nationwide. The ROCÍO (Rejilla Observacional con Interpolación Óptima) method (Rodríguez et al., 2003) was used to interpolate station observations into a 5 km gridded dataset, applying optimal interpolation and built-in AEMET quality control checks (e.g., internal consistency, temporal coherence, and range filtering).

2.5. Quality assurance and quality control (QA/QC)

QA/QC procedures were applied to all datasets and model outputs to ensure methodological representativeness and reliability (Figure S6).

To evaluate the stability of the wheat yield data, we implemented a bootstrap resampling procedure for each autonomous community following the approach described by Toma et al. (2017). This analysis confirmed that the dataset was statistically representative for every region during the study period.

$ET_{c\ act}$ retrieved from the TSEB model using MODIS Aqua and ERA5 was validated against 11 eddy covariance (EC) flux towers from the FLUXNET2015 and ICOS Warm Winter 2020 datasets. The EC data was filtered to retain days with mean energy balance closure of approximately 1. The comparison yielded a mean bias of 1.16 $mm.day^{-1}$, an average root mean square error (RMSE) of 1.76 $mm.day^{-1}$ and a correlation coefficient (r) of 0.52. Detailed evaluations are presented in the supplementary material (Figure S3 and Tabel S1).

To ensure reliable estimation of $ET_{c\ act}$, high-end biophysical

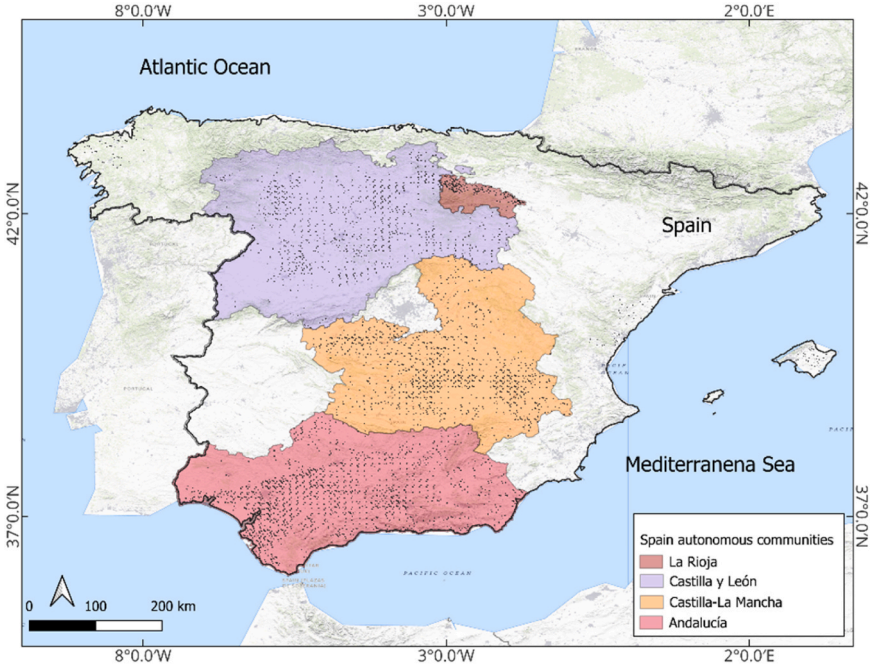

Fig. 1. Study area location of the four selected Spanish autonomous communities with spatial distribution of wheat dataset (black dots).

variables such as LAI and FPAR from the MODIS LAI/FPAR Collection 6 product were used (Yan et al., 2016). Temporal gap-filling and residual noise removal were applied on vegetation indices using TIMESAT Savitzky–Golay filtering method and the quality control layers embedded in MODIS products (Eklundh and Jönsson, 2017) and following (Gao et al., 2008) methodology, thus improving the reliability of satellite-derived vegetation metrics.

ET_o was computed using the FAO-56 Penman–Monteith (PM) formulation (Allen et al., 1998) with ERA5 meteorological data (incoming shortwave radiation, air temperature, actual water vapor pressure, atmospheric pressure and wind speed). Incoming shortwave radiation was corrected using a digital elevation model (DEM) and the MODIS MCD19A2 aerosol optical depth product. Solar zenith angle was derived from MODIS Aqua acquisition times to compute instantaneous shortwave radiation and ET_o, which were upscaled to daily values (Bozorgi et al., 2024). The reliability of ERA5-derived ET_o was evaluated against 16 weather station observations in Spain (Figure S2).

Assessing ERA5-derived ET_o against weather stations showed a mean bias of 0.36 $mm.day^{-1}$, an RMSE of 0.84 $mm.day^{-1}$ and r of 0.95 (Figure S4). These results compare well with previous evaluations of ERA5-based ET_o across diverse climatic regions reported RMSE values of 0.57–0.90 $mm.day^{-1}$ (Vanella et al., 2022; Ippolito et al., 2024; Xu et al., 2024).

The accuracy of wind speed from ERA5, previously identified as the variable with the largest bias (Aguirre-García et al., 2021; Vanella et al., 2022), was evaluated against weather stations indicated a mean bias of -2.31 $m{\cdot}s^{-1}$, an average RMSE of 3.22 $m{\cdot}s^{-1}$, and r of 0.65 (Figure S5).

The ROCIO daily precipitation dataset was previously validated against 64 independent meteorological stations, yielding a mean RMSE < 4 $mm.day^{-1}$ and a bias near 0 $mm.day^{-1}$ (Peral García et al., 2017), confirming its reliability for regional-scale hydrological analyses.

2.6. Drought indices

2.6.1. Standardized precipitation-evapotranspiration index (SPEI)

The Standardized Precipitation-Evapotranspiration Index (SPEI) developed by Vicente-Serrano et al. (2010), incorporates precipitation (P) and ET_o retrieved from ERA5 data to represent climatic water balance anomalies. The index is calculated as the difference between monthly precipitation and ET_o. SPEI has been widely applied in evaluating drought impacts on crop yields (Peña-Gallardo et al., 2019; Sosa et al., 2025; Tian et al., 2018; Vicente-Serrano et al., 2012; Zhao et al., 2023).

2.6.2. Standardized precipitation-actual evapotranspiration (SPET)

The Standardized Precipitation-Actual Evapotranspiration Index (SPET) developed by Padrón et al. (2020) assesses drought by computing anomalies in the difference between precipitation and $ET_{c\ act}$ retrieved from remote sensing data. Numerous studies have highlighted the strong link between $ET_{c\ act}$ and crop productivity (Bellvert et al., 2025; Tadesse et al., 2015), underscoring its importance in assessing drought impacts.

2.6.3. Standardized evapotranspiration deficit index (SEDI)

The Standardized Evapotranspiration Deficit Index (SEDI) developed by Vicente-Serrano et al. (2018) quantifies crop water stress based on the standardized monthly water balance as the difference between $ET_{c\ act}$ and ET_o. This formulation, also expressed as an $ET_{c\ act}/ET_o$ ratio, has been widely used to assess plant water stress and drought impacts (Anderson et al., 2016; Jurečka et al., 2021; Kim and Rhee, 2016; Mishra et al., 2013; Sepulcre-Canto et al., 2014; Stephenson, 1998).

2.6.4. Drought indices calculation

To identify the most responsive drought index for each region and to capture the influence of antecedent precipitation and soil-moisture conditions on wheat yield, drought indices were calculated at 1- to 12-month timescales over a harvest-to-harvest, ranging from the 1-month timescale in August to the 12-month timescales in July. Additionally, to ensure statistical robustness, all indices were fitted to a three-parameter log-logistic distribution following (Beguería et al., 2014; Vicente-Serrano et al., 2010). The cumulative distribution function of the log-logistic distribution is:

$$f(x) = \left[1 + \left[\frac{\alpha}{x - y}\right]^{\beta}\right]^{-1} \quad (1)$$

where x represents the water-balance series (D), and α, β and y are the scale, shape and location parameters that are estimated from data.

The D series for each index were computed as:

$$D_{SPEI} = P - ET_o \quad (2)$$

$$D_{SPET} = P - ET_{cact} \quad (3)$$

$$D_{SEDI} = ET_{cact} - ET_o \quad (4)$$

Standardized values were obtained using the classical Abramowitz–Stegun approximation to the standard normal distribution, following Vicente-Serrano et al. (2010). All drought index calculations were performed in RStudio.

2.7. Correlation analysis

To isolate the climatic effects in yield variations, the yield time series were detrended to remove the effects of non-climatic factors such as technological improvements and increased mechanization (Potopová et al., 2015; Tian et al., 2018), following (Lobell et al., 2011). For each community i, a quadratic polynomial trend was fitted to the time series of observed wheat yield (Eq. 5):

$$y'_{iT} = y_{it} - \hat{y}_{it} \quad (5)$$

where y'_{iT} is detrended yield, y_{it} is the observed yield, and $\hat{y}_{it}$ is the mean of fitted value from the quadratic polynomial trend model.

The standardized yield residual series (SYRS) was then derived using Eq. 6:

$$SYRS = \frac{y'_{iT} - \mu_i}{\delta_i} \quad (6)$$

where, μ_i and δ_i are the mean and standard deviation, respectively, of detrended yield for the community i.

The yield data was tested for normality using the Kolmogorov–Smirnov (K–S) test (Reschenhofer, 1997). Since the yield data did not meet the assumption of normality distribution, the non-parametric Spearman's rank correlation coefficient (ρ) was employed to quantify the correlation between drought indices and SYRS (Eq. 7):

$$\rho = 1 - \frac{6\sum d_i^2}{n(n^2 - 1)} \quad (7)$$

where d_i represents the difference in rank between paired observations and n is the total number of observations. The statistical correlation significance was set at the 95 % level.

3. Results

3.1. Statistical distribution of wheat yield

Bootstrapping confirmed adequate representativeness of the available data for all four study regions. The empirical cumulative distribution functions (ECDFs) of standardized wheat yield residuals across La Rioja, Castilla y León, Castilla-La Mancha, and Andalucía (Fig. 2) revealed marked inter-regional differences in yield variability. Andalucía displayed flatter ECDFs, indicating wider yield variability likely

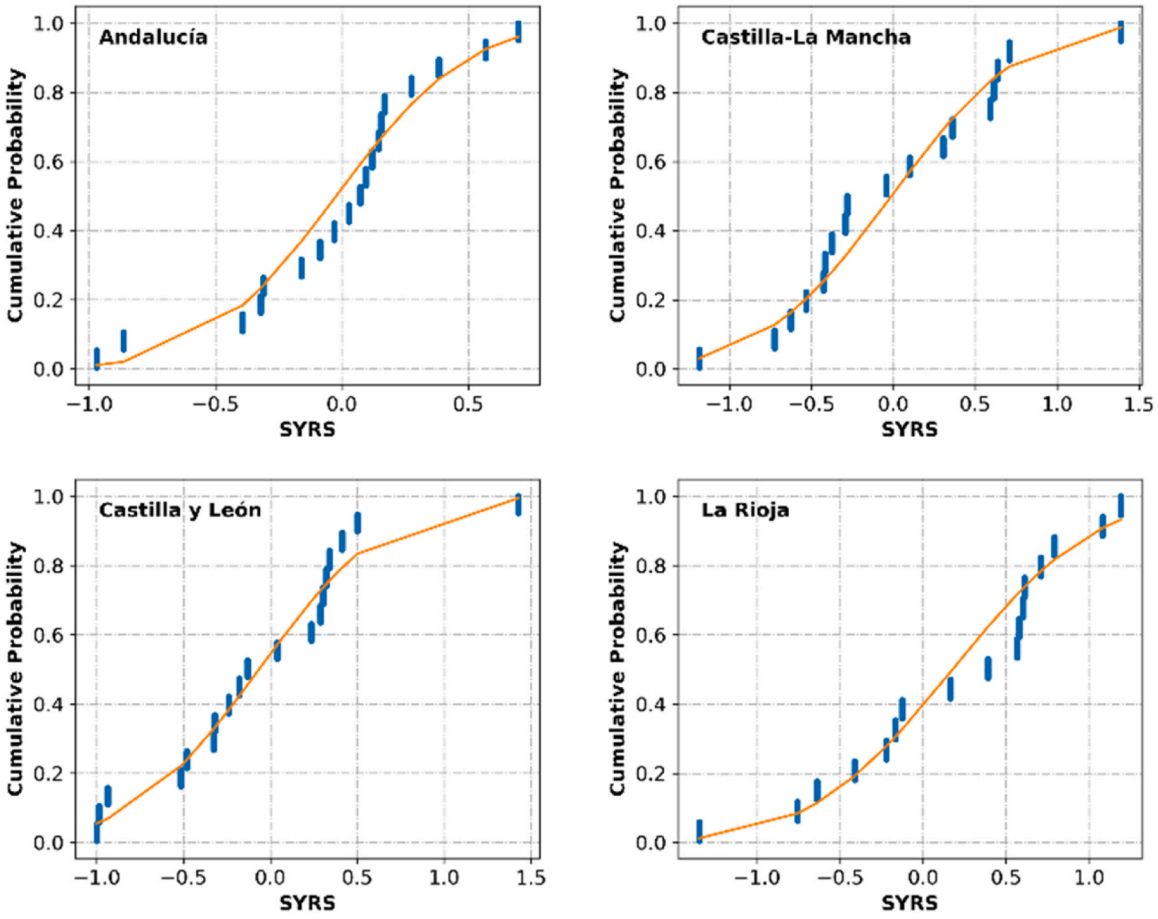

Fig. 2. Yield distribution for the period 2003–2021 within each selected autonomous community in Spain.

driven by climatic events and episodic droughts, whereas Castilla-La Mancha and Castilla y León exhibited steeper slopes reflecting more stable yield productivity.

The Kolmogorov–Smirnov (K–S) test rejected the null hypothesis of normality distribution for all regions ($p < 0.05$). This statistical asymmetry made it necessary to use non-parametric and distribution-free approaches in evaluating yield–drought interactions across Spanish zones.

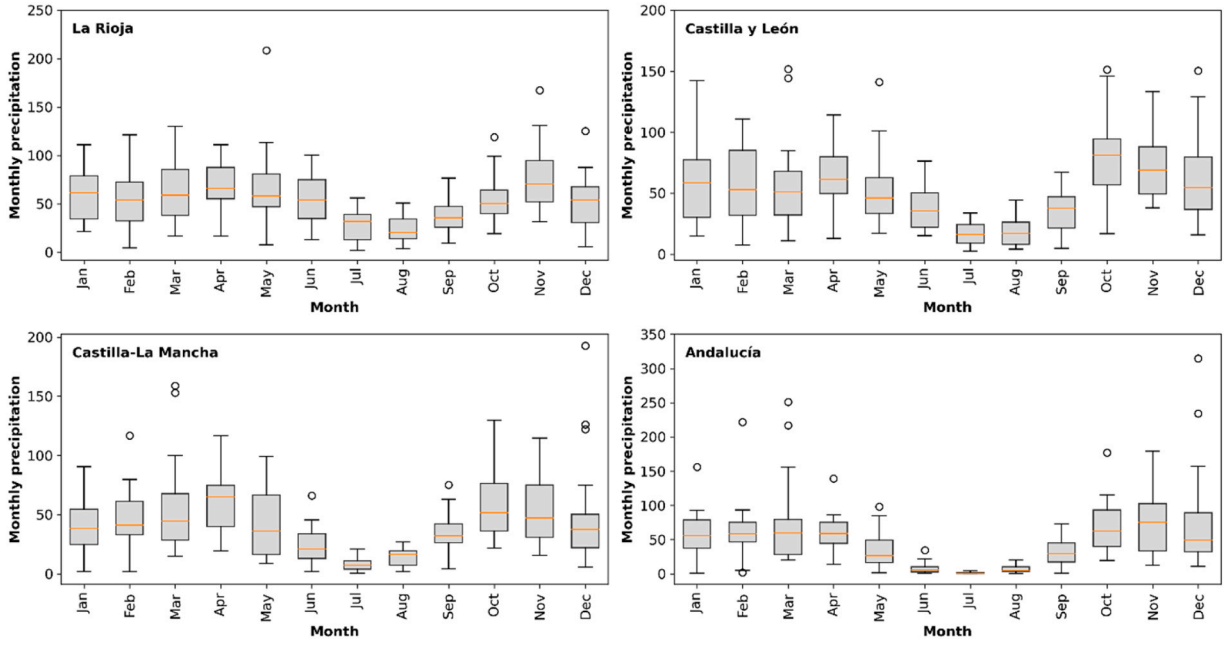

Fig. 3. Boxplot of monthly precipitation for the period 2003–2021 within the selected autonomous community in Spain.

3.2. Spatial patterns of interannual precipitation variability

The temporal variability of precipitation across four Spanish autonomous communities—La Rioja, Castilla y León, Castilla-La Mancha, and Andalucía—revealed pronounced seasonal patterns (Fig. 3), with notably lower precipitation during the summer (June–August) and higher levels during spring (March–May) and late autumn (October and November).

Andalucía displayed the greatest interannual variability by a large spread and frequency of outliers, indicating recurrent alternation between anomalously dry and wet years. This pattern reflected the region's exposure to hydrological extremes such as prolonged droughts and episodic flooding. Conversely, La Rioja showed relatively stable precipitation distribution with fewer extreme values, indicating a more moderate hydroclimate regime. The pronounced north–south gradient in precipitation variability underscored the spatial heterogeneity of Spain's hydroclimatic regimes, emphasizing the need for spatially explicit drought-impact assessment and region-specific agricultural water management strategies.

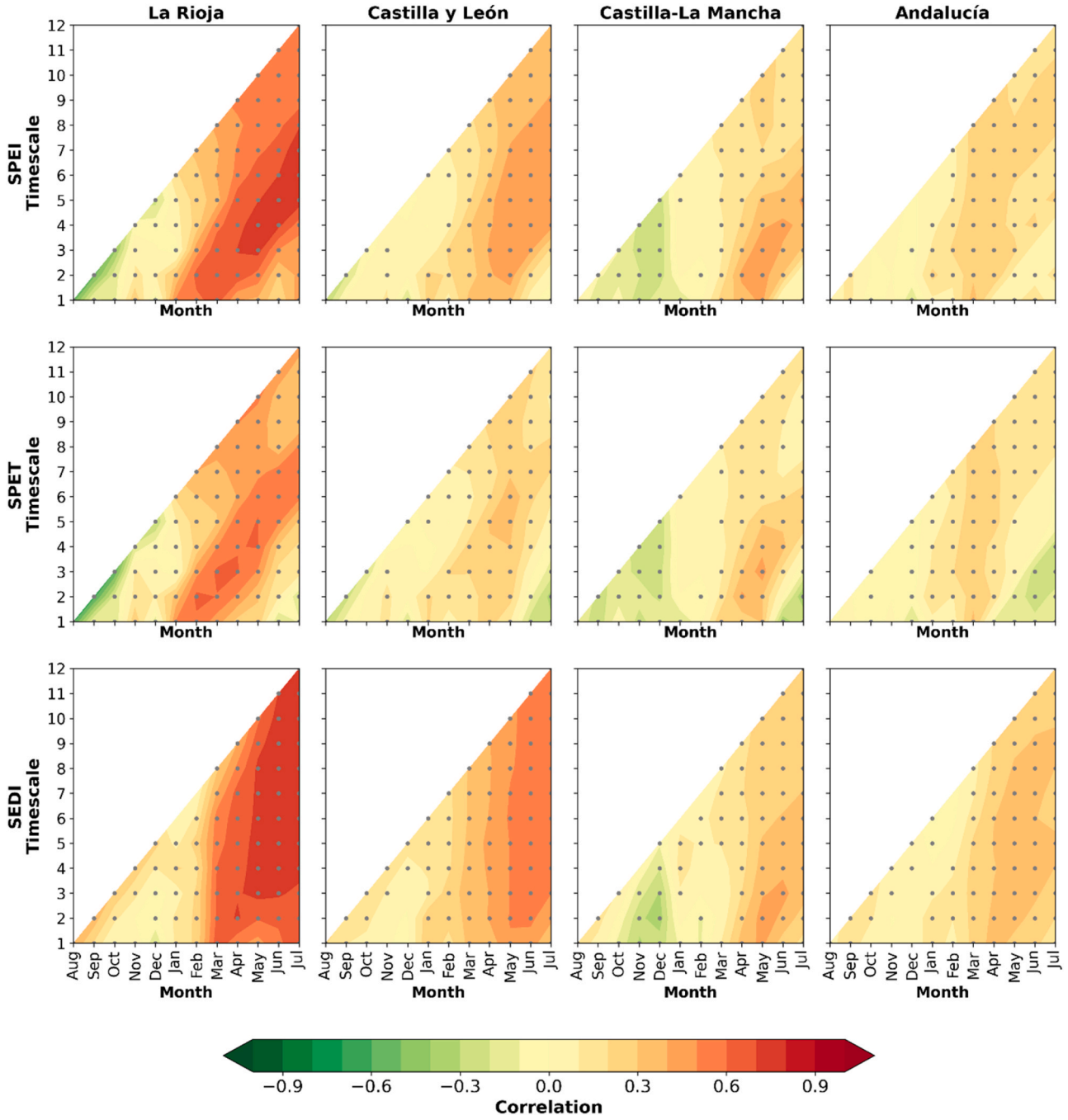

Fig. 4. Correlation patterns of the standardized wheat yield residuals series (SYRS) for the period 2003–2021 with SPEI, the standardized precipitation-evapotranspiration index; SPET, the standardized precipitation-actual evapotranspiration index; and SEDI, the standardized evapotranspiration deficit index, in 1–12 month timescales within each selected autonomous community in Spain. The color scale represents Spearman's correlation, and the dots show statistically significant correlations at the 95 % significant level ($p < 0.05$).

3.3. Spatial and temporal patterns of drought–wheat yield response

Drought–yield relationships exhibited clear spatial and temporal heterogeneity across Spain's main wheat-producing regions (Fig. 4). In Mediterranean areas such as Andalucía and Castilla-La Mancha, yield variability is most correlated at short timescales (1–3-month accumulation) peaking in late spring. In contrast, in more temperate continental regions (Castilla y León and La Rioja), yield variability correlated more strongly with longer drought periods (3–6-month accumulation) in early summer. These patterns highlight the need for region-specific drought monitoring strategies that account for local climatic regimes and agronomic heterogeneity.

Among the four regions, La Rioja displayed the highest correlations between drought indices and yield, with $r = 0.81$ for SEDI (July, six-month timescale), $r = 0.79$ for SPEI (July, seven-month timescale), and $r = 0.62$ for SPET (February, two-month timescale). The consistent performance of all indices likely reflects the relatively homogeneous climatic and land management conditions of this region. In Castilla y León, notable correlations were observed for SEDI in June ($r = 0.54$, three-month timescale), SPEI in July ($r = 0.51$, five-month timescale), and SPET in May ($r = 0.36$, six-month timescale). In northern Spain, SEDI generally more outperformed other indices, suggesting that integrating biophysical and climate variables—such as solar radiation, vapor pressure, and wind speed—enhances crop water availability estimation and yield-drought response.

In Castilla-La Mancha, the strongest relationships ($r = 0.45$–0.49)

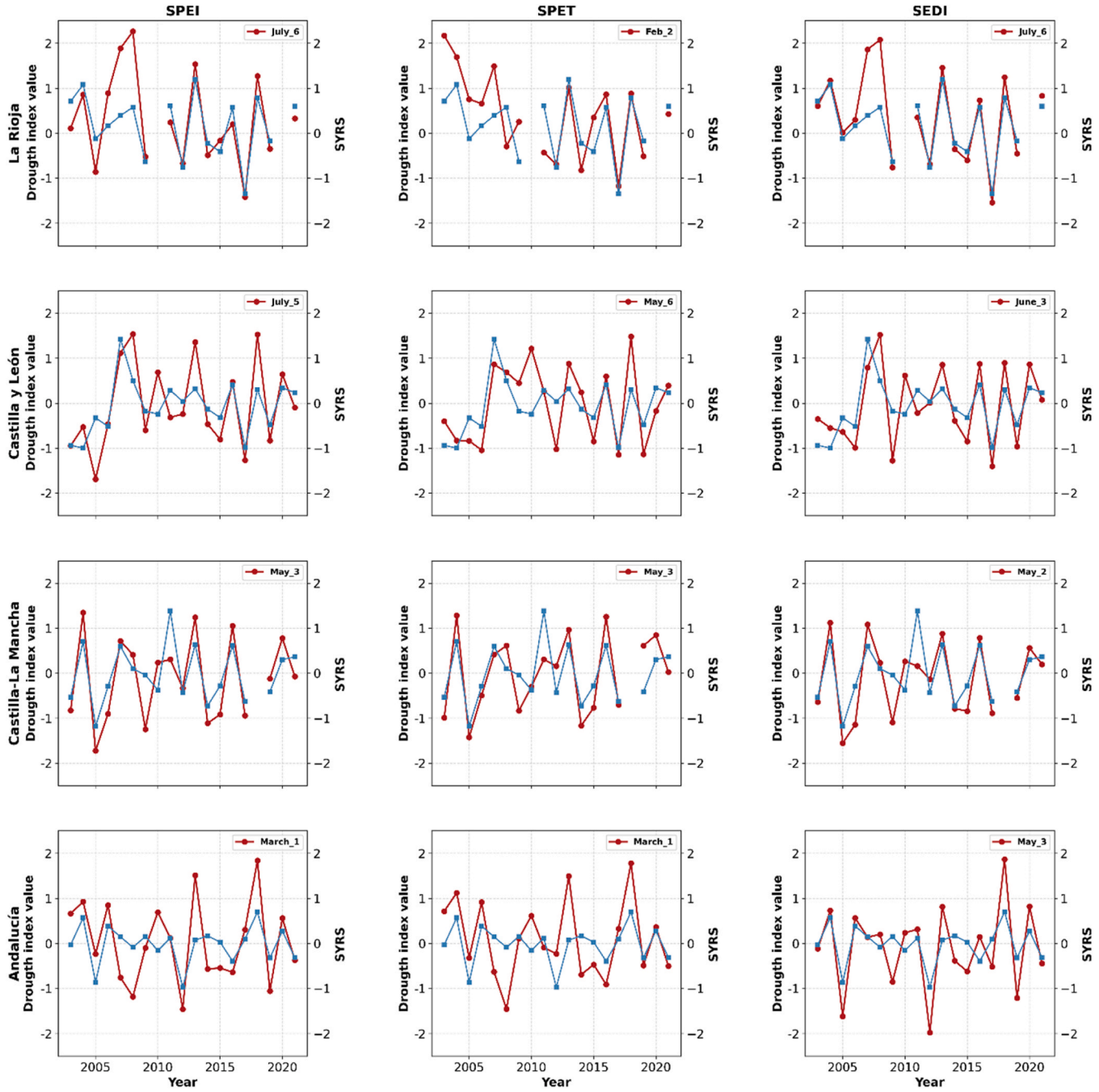

Fig. 5. Time series of SPEI, the standardized precipitation-evapotranspiration index; SPET, the standardized precipitation-actual evapotranspiration index; SEDI, the standardized evapotranspiration deficit index; and the standardized wheat yield residuals series (SYRS) for the period 2003–2021 in each selected autonomous community. The blue lines show SYRS, and the red lines show the drought index values.

occurred for SEDI in May (two-month timescale) and for SPEI and SPET in May (three-month timescale), indicating limited differentiation among indices. This suggests that additional variables, such as soil properties or agricultural management, may be required to better represent crop water stress in this semi-arid region. Similarly, in Andalucía, correlations were relatively weak ($r = 0.33$–0.35), peaking for SPEI and SPET in March (one-month timescale) and for SEDI in May (three-month timescale). These results from high spatial variability in cropping systems, cultivars, and management practices, which obscure direct drought–yield linkages.

3.4. Drought-wheat yield interannual variation

The interannual variation of the drought indices and wheat yield was shown in Fig. 5, based on the highest correlations observed in Fig. 4 in each drought index.

Temporal co-variation between drought indices and wheat yield demonstrated that all indices captured interannual yield fluctuations to varying degrees. In La Rioja, yield reductions in 2009, 2012, and 2017 were well represented by all indices, with SEDI providing the most accurate estimation of yield loss magnitude. However, in 2007 and 2008, drought indices indicated extremely wet conditions (values $> +1.5$), while yield anomalies were only moderately positive (~ 0.5), suggesting that non-climatic limitations—such as disease and pest—may have constrained yield potential during those years.

In Castilla y León, yield deficits observed in 2003, 2004, and 2017 closely corresponded with negative drought index values, with SEDI outperforming in capturing both the occurrence and severity of drought-induced yield reductions.

In Castilla-La Mancha, drought indices effectively reflected yield losses during 2003, 2005, and 2017, with SEDI best reproducing both the direction and magnitude of yield variability. Nevertheless, in years such as 2009 and 2011, all indices failed to represent observed yield anomalies, implying that additional agronomic information, particularly soil fertility, can improve wheat-yield response accuracy.

In Andalucía, negative yield anomalies in 2005, 2012, 2019, and 2021 coincided with negative signals in all drought indices, although the magnitude of yield loss was only moderately reproduced. This reduced correlation likely reflects the region's pronounced heterogeneity in management practices, soil conditions, and cultivar selection, which can obscure direct climate–yield linkages.

Regional differences in the agreement between drought indices and wheat yield can be attributed to climatic contrasts. La Rioja and Castilla y León experience humid-subtropical and warm-summer Mediterranean climates, where precipitation and temperature variability jointly regulate crop water availability. Conversely, Andalucía and Castilla-La Mancha are dominated by hot-summer Mediterranean and semi-arid conditions, where crop water stress interacts with management and cultivar differences. These climatic and agronomic disparities largely explain the heterogeneous drought–yield responses observed across Spain and emphasize the need for region-specific drought impact assessments for agricultural water management.

4. Discussion

4.1. Monitoring regional drought dynamics and implications for agricultural water management

Regional heterogeneity between drought indices and wheat yield underscored the necessity of spatially explicit agricultural drought monitoring and adaptive agricultural water management across Spain's diverse agroclimatic regions. The distinct climatic gradients -from the humid temperate north to the semi-arid south- generate contrasting yield response to agricultural drought.

In the northern temperate zones, yield variability was strongly coupled with hydroclimatic drivers, suggesting that drought indices can effectively serve as proxies for agricultural drought monitoring. These findings align with a previous study (Peña-Gallardo et al., 2019) that showed strong correlations between drought indices and yield in the north and central Spain. Therefore, understanding climate-driven yield variability provides a valuable foundation for enhancing yield prediction models and informing strategic agricultural management decisions in these regions.

Conversely, southern semi-arid regions (Andalucía and Castilla-La Mancha) exhibited weaker yield–drought correlation, highlighting the dominance of management and cultivar selection. The prevalence of extreme precipitation events in these areas further complicates water management. These hydroclimatic irregularities amplify yield variability and necessitate proactive soil moisture monitoring networks, irrigation optimization, and drought forecasting in these areas.

The superior performance of SEDI, particularly in northern Spain, demonstrates that remote sensing–derived $ET_{c\ act}$ can capture the actual crop water availability and crop water stress. SEDI integrates remotely sensed $ET_{c\ act}$ with ERA5 reanalysis data, thereby providing a more direct measure of agricultural drought intensity. This aligns with the findings of Bellvert et al. (2025) who emphasized the potential of remote sensing and $ET_{c\ act}$ for monitoring crop water deficits in Mediterranean agroecosystems. However, this study advances previous research by identifying long-term yield–drought interactions across multiple agroclimatic zones revealed the spatially explicit of wheat yield responses to drought, demonstrating that regional differences significantly influence the magnitude and distribution of drought impacts on wheat yield.

Additionally, while previous studies identified May–June as a high-risk period for drought impacts on cereal crops (Khlif et al., 2023), our results show that the accumulation timescales-not only the calendar month- critically determines yield response to drought which was varied regionally. In Andalusia and Castilla-La-Mancha yield variability was most strongly correlated with short timescales that peak in late spring (1–3-month accumulation; Fig. 4), whereas in Castilla y León and La Rioja the strongest correlations occurred for longer timescales, in early summer (3–6-month accumulation; Fig. 4). These contrasting timescales are consistent with regional differences in wheat phenology and growing-season length. These findings are consistent with Peña-Gallardo et al. (2019), which demonstrated that wheat yield is particularly vulnerable to spring droughts across Spain at both short (1–3 months) and medium (4–6 months) timescales.

This insight reinforces the need for dynamic drought monitoring systems leveraging remote sensing to deliver continuous spatiotemporal data. Such systems are essential for enabling policymakers and farm managers to transition from reactive drought responses toward anticipatory, risk-based decision-making frameworks.

Ultimately, the study contributes to a refined understanding of spatially differentiated drought–yield relationships across Spain, offering region-specific drought mitigation strategies and adaptive agricultural water management under climate change.

4.2. Integration of drought indices into yield prediction and crop modelling frameworks

Drought indices demonstrate the capacity to explain spatial and temporal variations in wheat yield, reinforcing their potential utility in yield prediction systems and crop modelling calibration. Given that drought remains the principal constraint on cereal production particularly in semi-arid Mediterranean agroecosystems (Asseng et al., 2015; Vadez et al., 2024), the spatial and temporal patterns identified in this study provide a foundation for improving both statistical and process-based yield prediction models.

Integrating drought indices—particularly SEDI—into crop models can enhance the parameterization of crop water stress functions and improve simulation accuracy under variable climatic regimes. Moreover, these indices can support early-warning systems that translate observed anomalies into yield forecasts, contributing directly to food

security and strategic water allocation planning.

The relationship between drought indices and yield variability is also shaped by factors that co-vary with water stress, including soil characteristics, nutrients, pest and disease pressure, and management intensity. These co-drivers are particularly influential in southern Spain, where more heterogeneous management regimes amplify the yield response to drought (Navarro-Cerrillo et al., 2022; Yang et al., 2024).

In this context, the study's results contribute to the operationalization of data-driven agricultural water management, bridging the gap between remote sensing science and decision-making.

4.3. Limitation and perspective

The coarse spatial resolution of both ET_o and $ET_{c\ act}$ products likely contributed to the low correlations observed between drought indices and wheat yield. $ET_{c\ act}$ derived from Aqua MODIS data at 1 km resolution introduces sub-pixel heterogeneity, as individual pixels may encompass multiple land-cover types. Consequently, $ET_{c\ act}$ estimates may represent aggregated evaporation and transpiration from mixed vegetation rather than crop-specific fluxes. To mitigate this trade-off, data-fusion techniques that combine the high spatial data from Landsat/Sentinel imagery with the temporal density of MODIS are recommended to improve $ET_{c\ act}$ estimation accuracy.

Meteorological forcing data with finer, agronomically relevant spatial resolution, particularly for wind speed, would further strengthen drought indices' performance. However, such high-resolution and continuous datasets are not yet available. As a result, ERA5 remains the only practical and consistent source for spatially explicit ET_o and drought indicators.

Additionall, incorporating sub-monthly drought indices (e.g., pentad or 10-day composites) might allow capturing flash droughts and heatwave impacts on crop productivity.

Finally, integrating information on soil characteristics, crop management practices, cultivar selection, and sowing and harvest dates will support region-specific analysis of drought impacts on wheat yield.

5. Conclusions

This study demonstrates that the Standardized Evapotranspiration Deficit Index (SEDI) provided the most robust and spatially consistent representation of drought–wheat yield relationships. Its strong performance highlights the effectiveness of integrating remotely sensed crop evapotranspiration ($ET_{c\ act}$) with ERA5 reanalysis data to produce continuous, spatially explicit drought monitoring, offering significant potential for advancing operational agricultural water management strategies.

Spatial analysis revealed pronounced geographical contrasts. In the northern regions, correlations between drought indices and wheat yields were consistently stronger. By contrast, the greater environmental and management variability across southern regions weakened these relationships, making drought impacts more difficult to discern. Such patterns highlight the inherent challenges of evaluating drought effects in heterogeneous dryland systems, underscoring the importance of concentrating analyses in areas with relatively uniform land characteristics, such as La Rioja, where drought–yield linkages can be identified with greater reliability.

Wheat-yield variability was most correlated to soil-moisture deficits from late winter to spring, but the relevant accumulation timescales differed by climate zone. Mediterranean regions such as Andalucía and Castilla-La Mancha responded to short timescales (1–3 months), whereas temperate continental regions including Castilla y León and La Rioja were influenced by longer timescales (3–6 months). These contrasting drought-wheat yield responses indicate that drought indicators must be region-specific to support accurate drought monitoring and water management strategies.

Future research should expand drought–yield assessment by incorporating higher spatial and temporal resolution of drought indices with soil characteristics, cultivar data, and sowing and harvest dates to better represent local agronomic drivers. Integrating these variables will further enhance the operational relevance of drought monitoring tools for climate-resilient agricultural water management.

Funding

This study was funded by the project ET4DROUGHT (No. PID2021–127345OR-C31) and DigiSPAC [TED2021–131237B-C21] both funded by the Ministry of Science and Innovation (MICIN-AEI).

CRediT authorship contribution statement

Mahsa Bozorgi: Writing – original draft, Software, Methodology, Conceptualization. **Jordi Cristóbal:** Writing – review & editing, Supervision, Methodology, Conceptualization. **Jaume Casadesús:** Writing – review & editing, Supervision.

Declaration of Competing Interest

The authors declare no conflicts of interest.

Acknowledgements

We would like to thank the *Ministerio de Agricultura, Pesca y Alimentación* of Spain for allowing us to use the Crop surface area and yields survey (ESYRCE) which has been crucial to develop this study. We would also like to acknowledge the *Sistema de Información Agroclimática para el Regadío* from the *Ministerio de Agricultura, Pesca y Alimentación* from Spain for the meteorological data provided by the *Sistema de Información Agroclimática para el Regadío* used in the ET_o evaluation.

Appendix A. Supporting information

Supplementary data associated with this article can be found in the online version at doi:10.1016/j.agwat.2025.110092.

Data availability

The authors do not have permission to share data.

References

Alatorre, L.C., Sánchez, E., Amado, J.P., Wiebe, L.C., Torres, M.E., Rojas, H.L., Bravo, L. C., López, E., López, E., 2015. Analysis of the temporal and spatial evolution of recovery and degradation processes in vegetated areas using a time series of landsat TM images (1986-2011): central region of Chihuahua, Mexico. Open J. 05. https://doi.org/10.4236/ojf.2015.52016.

Allen, R.G., Pereira, L.S., Raes, D., Smith, M., 1998. Crop evapotranspiration: Guidelines for computing crop requirements. In: Irrigation and Drainage Paper No, 56. FAO. https://doi.org/10.1016/j.eja.2010.12.001.

Anderson, M.C., Hain, C., Wardlow, B., Pimstein, A., Mecikalski, J.R., Kustas, W.P., 2011. Evaluation of drought indices based on Thermal remote sensing of evapotranspiration over the continental United States. J. Clim. 24. https://doi.org/10.1175/2010JCLI3812.1.

Anderson, M.C., Zolin, C.A., Sentelhas, P.C., Hain, C.R., Semmens, K., Tugrul Yilmaz, M., Gao, F., Otkin, J.A., Tetrault, R., 2016. The Evaporative Stress Index as an indicator of agricultural drought in Brazil: an assessment based on crop yield impacts. Remote Sens. Environ. 174. https://doi.org/10.1016/j.rse.2015.11.034.

Asseng, S., Ewert, F., Martre, P., Rötter, R.P., Lobell, D.B., Cammarano, D., Kimball, B.A., Ottman, M.J., Wall, G.W., White, J.W., Reynolds, M.P., Alderman, P.D., Prasad, P.V. V., Aggarwal, P.K., Anothai, J., Basso, B., Biernath, C., Challinor, A.J., De Sanctis, G., Doltra, J., Fereres, E., Garcia-Vila, M., Gayler, S., Hoogenboom, G., Hunt, L.A., Izaurralde, R.C., Jabloun, M., Jones, C.D., Kersebaum, K.C., Koehler, A.K., Müller, C., Naresh Kumar, S., Nendel, C., O'leary, G., Olesen, J.E., Palosuo, T., Priesack, E., Eyshi Rezaei, E., Ruane, A.C., Semenov, M.A., Shcherbak, I., Stöckle, C., Stratonovitch, P., Streck, T., Supit, I., Tao, F., Thorburn, P.J., Waha, K., Wang, E., Wallach, D., Wolf, J., Zhao, Z., Zhu, Y., 2015. Rising temperatures reduce global wheat production. Nat. Clim. Chang 5. https://doi.org/10.1038/nclimate2470.

Beguería, S., Vicente-Serrano, S.M., Reig, F., Latorre, B., 2014. Standardized precipitation evapotranspiration index (SPEI) revisited: parameter fitting,

evapotranspiration models, tools, datasets and drought monitoring. Int. J. Climatol. 34. https://doi.org/10.1002/joc.3887.
Bellvert, J., Pamies-Sans, M., Casadesús, J., Girona, J., 2025. Evaluating the impact of drought and water restrictions on agricultural production in irrigated areas through crop water productivity functions and a remote sensing-based evapotranspiration model. Agric. Water Manag 309, 109319. https://doi.org/10.1016/j.agwat.2025.109319.
Benito-Verdugo, P., Martínez-Fernández, J., González-Zamora, Á., Almendra-Martín, L., Gaona, J., Herrero-Jiménez, C.M., 2023. Impact of agricultural drought on barley and wheat yield: a comparative case study of Spain and Germany. Agriculture 13. https://doi.org/10.3390/agriculture13112111.
Bozorgi, M., Cristóbal, J., Pàmies-Sans, M., 2024. Evaluating the two-source energy balance model using MODIS data for estimating evapotranspiration time series on a regional scale. Remote Sens. 16. https://doi.org/10.3390/rs16234587.
Brown, J.F., Wardlow, B.D., Tadesse, T., Hayes, M.J., Reed, B.C., 2008. The vegetation drought response index (VegDRI): a new integrated approach for monitoring drought stress in vegetation. GIsci Remote Sens. 45. https://doi.org/10.2747/1548-1603.45.1.16.
Curtis, B.C., 2019. Wheat in the world. ⟨http://www.fao.org/3/y4011e/y4011e04.htm#TopOfPage⟩. Food and Agriculture Organisation of the United Nations 1–15.
Eklundh, L., Jönsson, P., 2017. TIMESAT 3.3 with seasonal trend decomposition and parallel processing Software Manual. Lund and Malmo University, Sweden.
European Environmental Agency (EEA), 2024. European climate risk assessment. Executive summary. EEA Report 01/2024. The European Climate Risk Assessment (EUCRA).
Gao, F., Morisette, J.T., Wolfe, R.E., Ederer, G., Pedelty, J., Masuoka, E., Myneni, R., Tan, B., Nightingale, J., 2008. An algorithm to produce temporally and spatially continuous MODIS-LAI time series. IEEE Geosci. Remote Sens. Lett. 5. https://doi.org/10.1109/LGRS.2007.907971.
García-León, D., Contreras, S., Hunink, J., 2019. Comparison of meteorological and satellite-based drought indices as yield predictors of Spanish cereals. Agric. Water Manag 213. https://doi.org/10.1016/j.agwat.2018.10.030.
Guttman, N.B., 1998. Comparing the palmer drought index and the standardized precipitation index. J. Am. Water Resour. Assoc. 34. https://doi.org/10.1111/j.1752-1688.1998.tb05964.x.
Heim, R.R., 2002. A review of twentieth-century drought indices used in the United States. Bull. Am. Meteor. Soc. https://doi.org/10.1175/1520-0477(2002)083<1149:AROTDI>2.3.CO;2.
Hu, T., van Dijk, A.I.J.M., Renzullo, L.J., Xu, Z., He, J., Tian, S., Zhou, J., Li, H., 2020. On agricultural drought monitoring in Australia using Himawari-8 geostationary thermal infrared observations. Int. J. Appl. Earth Obs. Geoinf. 91. https://doi.org/10.1016/j.jag.2020.102153.
Ippolito, M., De Caro, D., Cannarozzo, M., Provenzano, G., Ciraolo, G., 2024. Evaluation of daily crop reference evapotranspiration and sensitivity analysis of FAO Penman-Monteith equation using ERA5-Land reanalysis database in Sicily, Italy. Agric. Water Manag. 295. https://doi.org/10.1016/j.agwat.2024.108732.
Jiménez-Donaire, M.D.P., Giráldez, J.V., Vanwalleghem, T., 2020. Impact of climate change on agricultural droughts in Spain. Water 12. https://doi.org/10.3390/w12113214.
Jurečka, F., Fischer, M., Hlavinka, P., Balek, J., Semerádová, D., Bláhová, M., Anderson, M.C., Hain, C., Žalud, Z., Trnka, M., 2021. Potential of water balance and remote sensing-based evapotranspiration models to predict yields of spring barley and winter wheat in the Czech Republic. Agric. Water Manag. 256. https://doi.org/10.1016/j.agwat.2021.107064.
Karl, T.R., 1986. The sensitivity of the Palmer Drought Severity Index and Palmer's Z-index to their calibration coefficients including potential evapotranspiration. J. Clim. Appl. Meteorol. 25. https://doi.org/10.1175/1520-0450(1986)025<0077:TSOTPD>2.0.CO;2.
Khlif, M., Escorihuela, M.J., Chahbi Bellakanji, A., Paolini, G., Lili Chabaane, Z., 2023. Remotely sensed agriculture drought indices for assessing the impact on cereal yield. Remote Sens. 15. https://doi.org/10.3390/rs15174298.
Kim, D., Rhee, J., 2016. A drought index based on actual evapotranspiration from the Bouchet hypothesis. Geophys. Res. Lett. 43. https://doi.org/10.1002/2016GL070302.
Wilhite, D.A. (Ed.), 2005. Drought and Water Crises. CRC Press. https://doi.org/10.1201/9781420028386.
Leng, G., Hall, J., 2019. Crop yield sensitivity of global major agricultural countries to droughts and the projected changes in the future. Sci. Total Environ. 654. https://doi.org/10.1016/j.scitotenv.2018.10.434.
Lobell, D.B., Di Tommaso, S., 2025. A half-century of climate change in major agricultural regions: trends, impacts, and surprises. Proc. Natl. Acad. Sci. 122, e2502789122. https://doi.org/10.1073/pnas.2502789122.
Lobell, D.B., Schlenker, W., Costa-Roberts, J., 2011. Climate trends and global crop production since 1980. Science 333, 1979. https://doi.org/10.1126/science.1204531.
Mahadevan, M., Noel, J.K., Umesh, M., Santhosh, A.S., Suresh, S., 2024. Climate Change Impact on Water Resources, Food Production and Agricultural Practices. In: Singh, P., Yadav, N. (Eds.), The Climate-Health-Sustainability Nexus: Understanding the Interconnected Impact on Populations and the Environment. Springer Nature Switzerland, Cham, pp. 207–229. https://doi.org/10.1007/978-3-031-56564-9_9.
Marengo, J.A., Torres, R.R., Alves, L.M., 2017. Drought in Northeast Brazil—past, present, and future. Theor. Appl. Clim. 129. https://doi.org/10.1007/s00704-016-1840-8.
Martínez-Moreno, F., Guzmán-Álvarez, J.R., Díez, C.M., Rallo, P., 2023. The Origin of Spanish Durum wheat and olive tree landraces based on genetic structure analysis and historical records. Agronomy. https://doi.org/10.3390/agronomy13061608.
McKee, T.B., Doesken, N.J., Kleist, J., 1993. The Relationship of Drought Frequency and Duration to Time Scales, in: 8th Conference on Applied Climatology. Anaheim, pp. 179–184.
Mishra, V., Cruise, J.F., Mecikalski, J.R., Hain, C.R., Anderson, M.C., 2013. A remote-sensing driven tool for estimating crop stress and yields. Remote Sens. 5. https://doi.org/10.3390/rs5073331.
Nalbantis, I., Tsakiris, G., 2009. Assessment of hydrological drought revisited. Water Resour. Manag. 23. https://doi.org/10.1007/s11269-008-9305-1.
Navarro-Cerrillo, R.M., González-Moreno, P., Ruiz-Gómez, F.J., Sánchez-Cuesta, R., Gazol, A., Camarero, J.J., 2022. Drought stress and pests increase defoliation and mortality rates in vulnerable Abies pinsapo forests. Ecol. Manag. 504. https://doi.org/10.1016/j.foreco.2021.119824.
OECD, 2025. Global Drought Outlook: Trends, Impacts and Policies to Adapt to a Drier World. OECD Publishing, Paris. https://doi.org/10.1787/d492583a-en.
Padrón, R.S., Gudmundsson, L., Decharme, B., Ducharne, A., Lawrence, D.M., Mao, J., Peano, D., Krinner, G., Kim, H., Seneviratne, S.I., 2020. Observed changes in dry-season water availability attributed to human-induced climate change. Nat. Geosci. 13. https://doi.org/10.1038/s41561-020-0594-1.
Palmer, W.C., 1965. Meteorological Drought. No. In: Office of Climatology Research Paper, 45. US Weather Bureau, Washington DC.
Peña-Gallardo, M., Martín Vicente-Serrano, S., Domínguez-Castro, F., Beguería, S., 2019. The impact of drought on the productivity of two rainfed crops in Spain. Nat. Hazards Earth Syst. Sci. 19. https://doi.org/10.5194/nhess-19-1215-2019.
Peng, L., Sheffield, J., Wei, Z., Ek, M., Wood, E.F., 2024. An enhanced standardized precipitation–evapotranspiration index (SPEI) drought-monitoring method integrating land surface characteristics. Earth Syst. Dyn. 15, 1277–1300. https://doi.org/10.5194/esd-15-1277-2024.
Perez, M., Lombardi, D., Bardino, G., Vitale, M., 2024. Drought assessment through actual evapotranspiration in Mediterranean vegetation dynamics. Ecol. Indic. 166, 112359. https://doi.org/10.1016/j.ecolind.2024.112359.
Possega, M., García-Valdecasas Ojeda, M., Gámiz-Fortis, S.R., 2023. Multi-scale analysis of agricultural drought propagation on the iberian peninsula using non-parametric indices. Water 15. https://doi.org/10.3390/w15112032.
Potopová, V., Štěpánek, P., Možný, M., Türkott, L., Soukup, J., 2015. Performance of the standardised precipitation evapotranspiration index at various lags for agricultural drought risk assessment in the Czech Republic. Agric. Meteor. 202. https://doi.org/10.1016/j.agrformet.2014.11.022.
Qiu, J., Shen, Z., Xie, H., 2023. Drought impacts on hydrology and water quality under climate change. Sci. Total Environ. 858. https://doi.org/10.1016/j.scitotenv.2022.159854.
Reschenhofer, E., 1997. Generalization of the Kolmogorov-Smirnov test. Comput. Stat. Data Anal. 24. https://doi.org/10.1016/S0167-9473(96)00077-1.
Ribeiro, A.F.S., Russo, A., Gouveia, C.M., Pascoa, P., Pires, C.A.L., 2019. Probabilistic modelling of the dependence between rainfed crops and drought hazard. Nat. Hazards Earth Syst. Sci. 19. https://doi.org/10.5194/nhess-19-2795-2019.
Rockström, J., Karlberg, L., Wani, S.P., Barron, J., Hatibu, N., Oweis, T., Bruggeman, A., Farahani, J., Qiang, Z., 2010. Managing water in rainfed agriculture-The need for a paradigm shift. Agric. Water Manag 97. https://doi.org/10.1016/j.agwat.2009.09.009.
Rodríguez, E., Navascués, B., Ayuso, J.J., Järvenoja, S., 2003. Analysis of surface variables and parameterization of surface processes in HIRLAM. Part I: approach and verification by parallel runs. HIRLAM Tech. Repport 58.
Schwartz, C., Ellenburg, W.L., Mishra, V., Mayer, T., Griffin, R., Qamer, F., Matin, M., Tadesse, T., 2022. A statistical evaluation of Earth-observation-based composite drought indices for a localized assessment of agricultural drought in Pakistan. Int. J. Appl. Earth Obs. Geoinf. 106. https://doi.org/10.1016/j.jag.2021.102646.
Sepulcre-Canto, G., Vogt, J., Arboleda, A., Antofie, T., 2014. Assessment of the EUMETSAT LSA-SAF evapotranspiration product for drought monitoring in Europe. Int. J. Appl. Earth Obs. Geoinf. 30. https://doi.org/10.1016/j.jag.2014.01.021.
Shukla, S., Wood, A.W., 2008. Use of a standardized runoff index for characterizing hydrologic drought. Geophys. Res. Lett. 35. https://doi.org/10.1029/2007GL032487.
Sosa, G., Fernández-Long, M.E., Vicente-Serrano, S.M., 2025. Evaluating the performance of drought indices for assessing agricultural droughts in Argentina. Agron. J. 117, e70008. https://doi.org/10.1002/agj2.70008.
Stagge, J.H., Kingston, D.G., Tallaksen, L.M., Hannah, D.M., 2017. Observed drought indices show increasing divergence across Europe. Sci. Rep. 7. https://doi.org/10.1038/s41598-017-14283-2.
Stagge, J.H., Tallaksen, L.M., Xu, C.Y., Van Lanen, H.A.J., 2014. Standardized precipitation-evapotranspiration index (SPEI): Sensitivity to potential evapotranspiration model and parameters, in: IAHS-AISH Proceedings and Reports.
Stephenson, N.L., 1998. Actual evapotranspiration and deficit: biologically meaningful correlates of vegetation distribution across spatial scales. J. Biogeogr. 25. https://doi.org/10.1046/j.1365-2699.1998.00233.x.
Sun, D., Zhang, H., Qi, Y., Ren, Y., Zhang, Z., Li, X., Lv, Y., Cheng, M., 2025. A comparative analysis of different algorithms for estimating evapotranspiration with limited observation variables: a case study in Beijing, China. Remote Sens. 17. https://doi.org/10.3390/rs17040636.
Tadesse, T., Senay, G.B., Berhan, G., Regassa, T., Beyene, S., 2015. Evaluating a satellite-based seasonal evapotranspiration product and identifying its relationship with other satellite-derived products and crop yield: A case study for Ethiopia. Int. J. Appl. Earth Obs. Geoinf. 40. https://doi.org/10.1016/j.jag.2015.03.006.
Tian, L., Yuan, S., Quiring, S.M., 2018. Evaluation of six indices for monitoring agricultural drought in the south-central United States. Agric. Meteor. 249. https://doi.org/10.1016/j.agrformet.2017.11.024.

Toma, P., Miglietta, P.P., Zurlini, G., Valente, D., Petrosillo, I., 2017. A non-parametric bootstrap-data envelopment analysis approach for environmental policy planning and management of agricultural efficiency in EU countries. Ecol. Indic. 83. https://doi.org/10.1016/j.ecolind.2017.07.049.

Vadez, V., Grondin, A., Chenu, K., Henry, A., Laplaze, L., Millet, E.J., Carminati, A., 2024. Crop traits and production under drought. Nat. Rev. Earth Environ. https://doi.org/10.1038/s43017-023-00514-w.

Vanella, D., Longo-Minnolo, G., Belfiore, O.R., Ramírez-Cuesta, J.M., Pappalardo, S., Consoli, S., D'Urso, G., Chirico, G.B., Coppola, A., Comegna, A., Toscano, A., Quarta, R., Provenzano, G., Ippolito, M., Castagna, A., Gandolfi, C., 2022. Comparing the use of ERA5 reanalysis dataset and ground-based agrometeorological data under different climates and topography in Italy. J. Hydrol. Reg. Stud. 42. https://doi.org/10.1016/j.ejrh.2022.101182.

Vicente-Serrano, S.M., Beguería, S., López-Moreno, J.I., 2010. A multiscalar drought index sensitive to global warming: the standardized precipitation evapotranspiration index. J. Clim. 23, 1696–1718. https://doi.org/10.1175/2009JCLI2909.1.

Vicente-Serrano, S.M., Beguería, S., López-Moreno, J.I., 2011. Comment on characteristics and trends in various forms of the Palmer Drought Severity Index (PDSI) during 1900-2008 by Aiguo Dai. J. Geophys. Res. Atmospheres. https://doi.org/10.1029/2011jd016410.

Vicente-Serrano, S.M., Beguería, S., Lorenzo-Lacruz, J., Camarero, J.J., López-Moreno, J. I., Azorin-Molina, C., Revuelto, J., Morán-Tejeda, E., Sanchez-Lorenzo, A., 2012. Performance of drought indices for ecological, agricultural, and hydrological applications. Earth Inter. 16. https://doi.org/10.1175/2012EI000434.1.

Vicente-Serrano, S.M., Beguería, S., 2016. Comment on "Candidate distributions for climatological drought indices (SPI and SPEI)" by James H. Stagge et al. International Journal of Climatology 36. https://doi.org/10.1002/joc.4474.

Vicente-Serrano, S., Cuadrat-Prats, J.M., Romo, A., 2006. Early prediction of crop production using drought indices at different time-scales and remote sensing data: application in the Ebro Valley (north-east Spain). Int J. Remote Sens 27. https://doi.org/10.1080/01431160500296032.

Vicente-Serrano, S.M., Gouveia, C., Camarero, J.J., Beguería, S., Trigo, R., López-Moreno, J.I., Azorín-Molina, C., Pasho, E., Lorenzo-Lacruz, J., Revuelto, J., Morán-Tejeda, E., Sanchez-Lorenzo, A., 2013. Response of vegetation to drought time-scales across global land biomes. Proc. Natl. Acad. Sci. USA 110. https://doi.org/10.1073/pnas.1207068110.

Vicente-Serrano, S.M., Miralles, D.G., Domínguez-Castro, F., Azorin-Molina, C., El Kenawy, A., Mcvicar, T.R., Tomás-Burguera, M., Beguería, S., Maneta, M., Peña-Gallardo, M., 2018. Global assessment of the standardized evapotranspiration deficit index (SEDI) for drought analysis and monitoring. J. Clim. 31. https://doi.org/10.1175/JCLI-D-17-0775.1.

Visser, M.A., Kumetat, G., Scott, G., 2024. Drought, water management, and agricultural livelihoods: understanding human-ecological system management and livelihood strategies of farmer's in rural California. J. Rural Stud. 109, 103339. https://doi.org/10.1016/j.jrurstud.2024.103339.

Wang, L., Ren, W., 2025. Drought in agriculture and climate-smart mitigation strategies. Cell Rep. Sustain., 100386 https://doi.org/10.1016/j.crsus.2025.100386.

Wen, Q., Tu, X., Zhou, L., Singh, V.P., Chen, X., Lin, K., 2025. Mutual-information of meteorological-soil and spatial propagation: Agricultural drought assessment based on network science. Ecol. Indic. 170, 113004. https://doi.org/10.1016/j.ecolind.2024.113004.

West, H., Quinn, N., Horswell, M., 2019. Remote sensing for drought monitoring & impact assessment: Progress, past challenges and future opportunities. Remote Sens. Environ. 232, 111291. https://doi.org/10.1016/j.rse.2019.111291.

Wilhite, D.A., Sivakumar, M.V.K., Pulwarty, R., 2014. Managing drought risk in a changing climate: the role of national drought policy. Weather Clim. Extrem 3. https://doi.org/10.1016/j.wace.2014.01.002.

Wilhite, D.A., Svoboda, M.D., 2000. Drought early warning systems in the context of drought preparedness and mitigation. Early warning systems for drought preparedness and drought management.

Wu, D., Li, Z., Zhu, Y., Li, X., Wu, Y., Fang, S., 2021. A new agricultural drought index for monitoring the water stress of winter wheat. Agric. Water Manag. 244. https://doi.org/10.1016/j.agwat.2020.106599.

Wu, B., Meng, J., Li, Q., Yan, N., Du, X., Zhang, M., 2014. Remote sensing-based global crop monitoring: experiences with China's CropWatch system. Int. J. Digit Earth. https://doi.org/10.1080/17538947.2013.821185.

Xu, S., Li, J., Zhang, T., 2024. Effects of drought on ecosystem evapotranspiration and gross primary productivity in the Haihe River Basin. Phys. Chem. Earth Parts A/B/C. 135, 103619. https://doi.org/10.1016/j.pce.2024.103619.

Xu, Z., Sun, H., Zhang, T., Xu, H., Wu, D., Gao, J., 2024. The high spatial resolution Drought Response Index (HiDRI): An integrated framework for monitoring vegetation drought with remote sensing, deep learning, and spatiotemporal fusion. Remote Sens. Environ. 312, 114324. https://doi.org/10.1016/j.rse.2024.114324.

Yan, K., Park, T., Yan, G., Liu, Z., Yang, B., Chen, C., Nemani, R.R., Knyazikhin, Y., Myneni, R.B., 2016. Evaluation of MODIS LAI/FPAR product collection 6. Part 2: validation and intercomparison. Remote Sens. 8. https://doi.org/10.3390/rs8060460.

Yang, K., Llusià, J., Preece, C., Ogaya, R., Márquez Tur, L., Mu, Z., You, C., Xu, Z., Tan, Y., Peñuelas, J., 2024. Impacts of seasonality, drought, nitrogen fertilization, and litter on soil fluxes of biogenic volatile organic compounds in a Mediterranean forest. Sci. Total Environ. 906. https://doi.org/10.1016/j.scitotenv.2023.167354.

Zampieri, M., Ceglar, A., Dentener, F., Toreti, A., 2017. Wheat yield loss attributable to heat waves, drought and water excess at the global, national and subnational scales. Environ. Res. Lett. 12. https://doi.org/10.1088/1748-9326/aa723b.

Zhao, H., Huang, Y., Wang, X., Li, X., Lei, T., 2023. The performance of SPEI integrated remote sensing data for monitoring agricultural drought in the North China Plain. Field Crops Res. 302. https://doi.org/10.1016/j.fcr.2023.109041.